

THE ROLE OF CONSTITUENT QUARK MASS IN THE STANDARD MODEL

- S.I.Sukhoruchkin
- Petersburg Nuclear Physics Institute, Gatchina, Russia

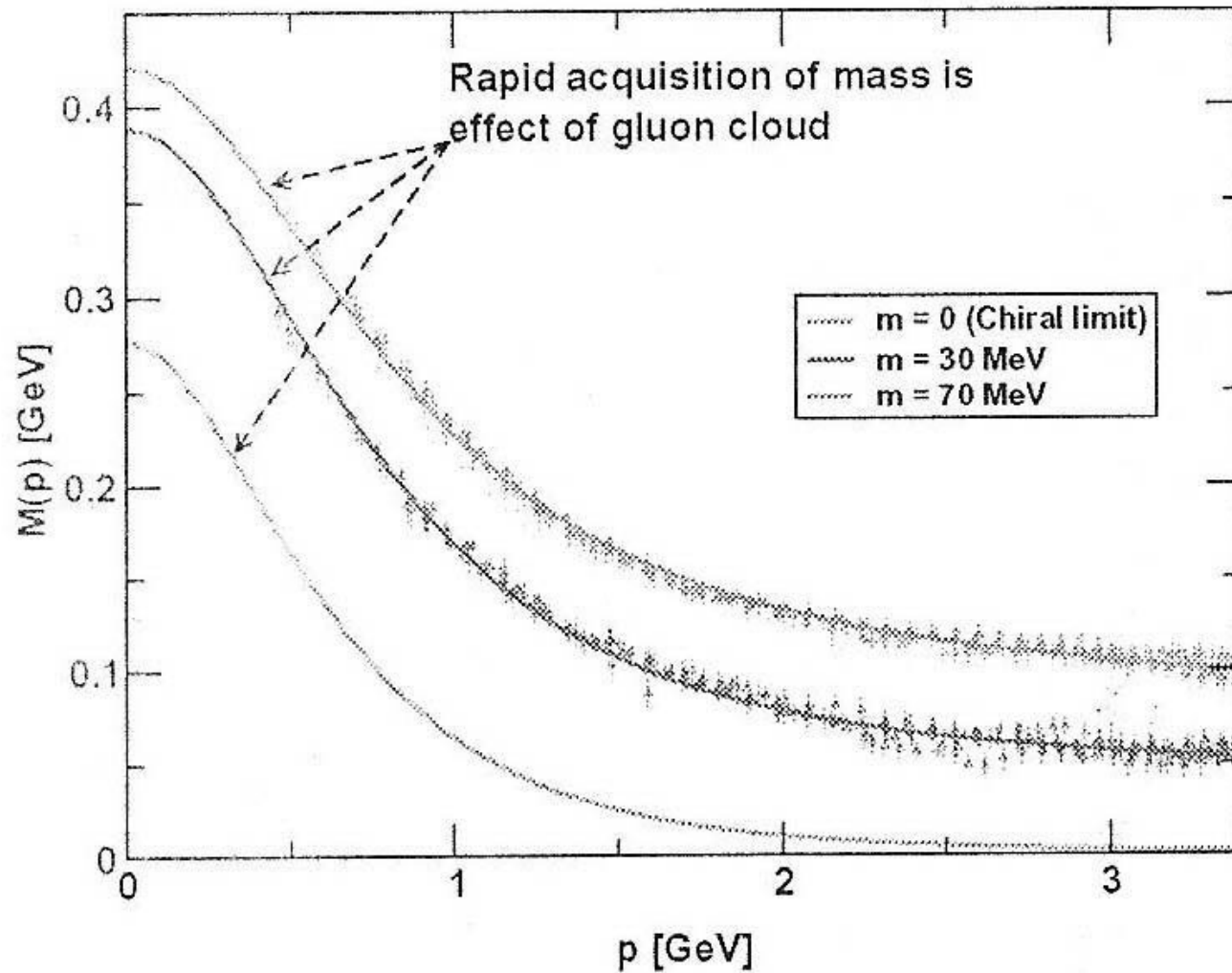


Fig.1. QCD gluon-quark-dressing effect calculated with Dyson-Schwinger Equation [9,13-17], initial masses $m=0, 30$ and 70 MeV; the constituent-quark mass arises from a cloud of low-momentum gluons attaching themselves to the current-quark; this is dynamical chiral symmetry breaking: a nonperturbative effect that generates a quark mass from nothing even at chiral limit $m=0$, bottom curve) [9].

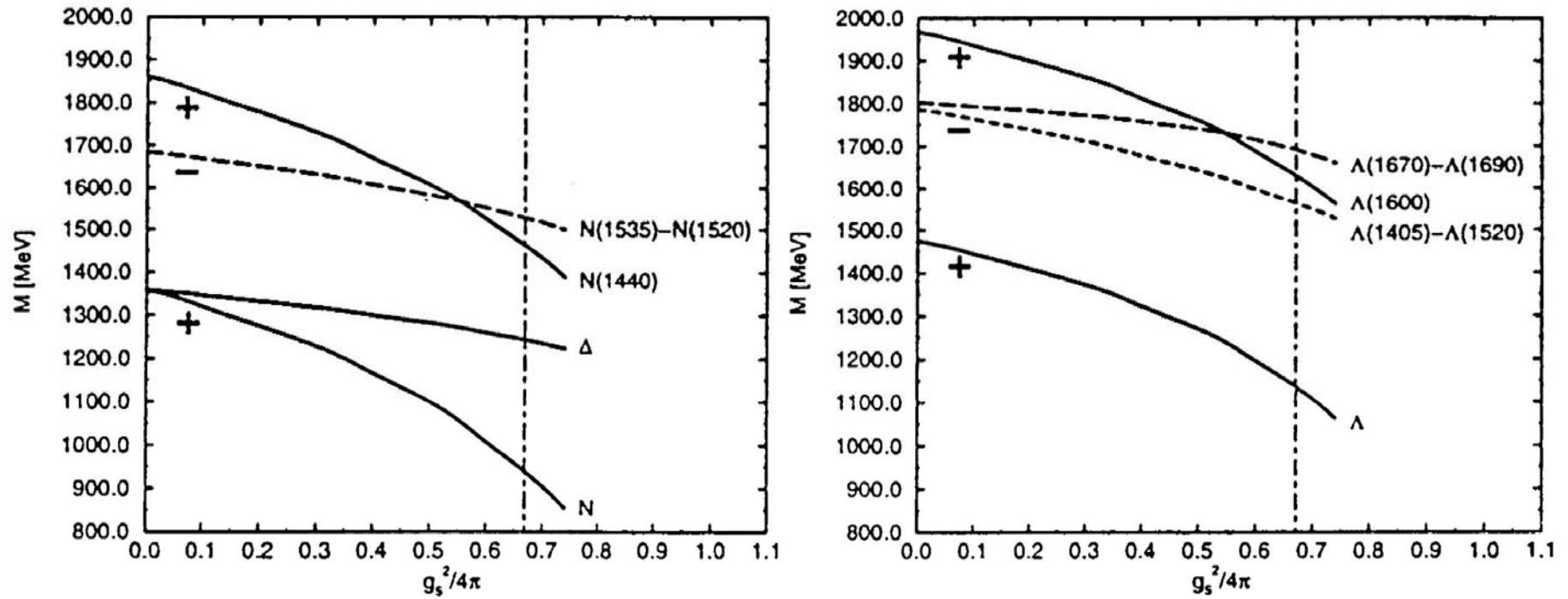


Fig.2. Calculation of nonstrange baryon masses (left) and Λ -hyperon masses as a function of interaction strength within GBECQM – Goldstone Boson Exchange interaction Constituent Quark Model [19]; initial baryon mass $1350 \text{ MeV} = 3 \times 450 \text{ MeV} = 3M_q$ is near the bottom "+" on the left vertical axis.

Table 1. Discussed in the literature closeness of masses or mass differences to the integer numbers (k) of the pion mass value $m_\pi^\pm=139.5$ MeV or to $2m_\pi^\pm+m_\pi^0=\kappa_T=409$ MeV.

Particle	Λ	Ω	(bb)(2S-1S)	(bb)(4S-2S)	ΔE_B
Mass or ΔM (MeV)	1115.683(6)	1672.45(29)	10023-9460	10579-10023	408.9
			=563	=556	
km_π or $2m_\pi^\pm+m_\pi^0=\kappa_T$	1116 k=8	1672 k=12	558 k=4	558 k=4	409 κ_T
difference, reference	0, [1,23-26]	0, [1,25,26]	-5, [1,26]	-2, [1,27]	0, [28]

Table 2. Discussed in the literature closeness of particle masses or mass differences to the integer numbers (k) of the nucleon Δ -excitation parameter $\Delta_\Delta=147$ MeV [23].

Particle	(cc) (2S-1S)	(cc) (1S)	Ξ^-	$\omega_3-\omega$	$K_3^*-K^*(892)$	ΔE_B
Mass or	3686.1-3096.9	3096.92(1)	1321.3	1667(4)-782.7	1776(7)-891.7	441.5 (Fig.4)
ΔM (MeV)	=589.2 k=4	3087 k=21	k=9	884(4) k=6	=884(7) k=6	k=4
$k\Delta M_\Delta$	588	588	1323	882	882	441
diff., ref.	1,[1,25,29]	1,[1,25,29]	-2,[??]	2(4),[1,25,29]	2(7),[1,25,29]	0,[28]

THE BOTTOMONIUM SYSTEM

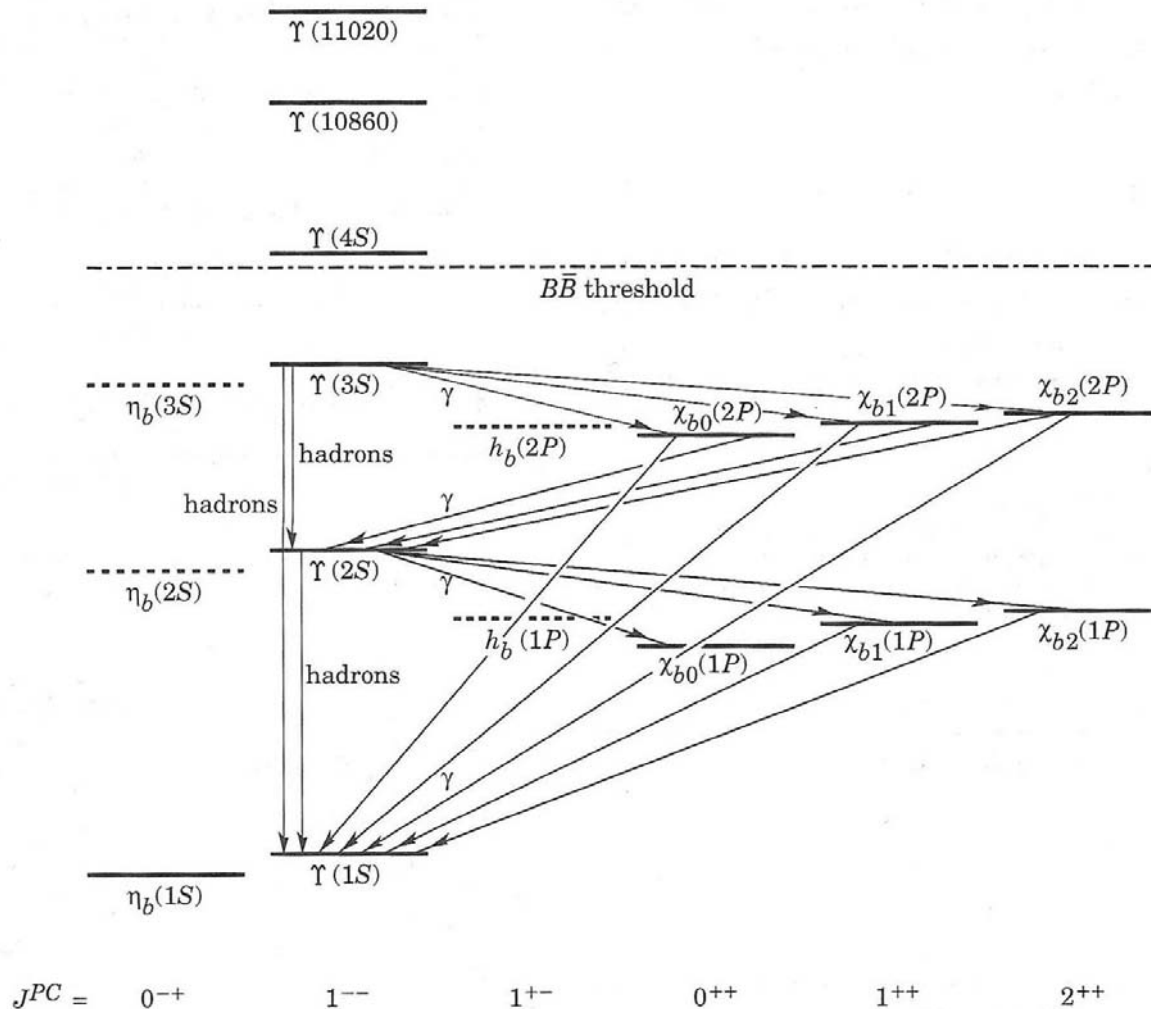


Fig.3. *Top* Mesons of (bb)-structure with radial excitations $n=1$ and $n=1-3$ close to $4m_\tau$ [1,27];
Bottom Mesons of (cc)-structure with radial excitation ($n=1$) close to $4\Delta M_\Delta=4\times 147\text{ MeV}=588\text{ MeV}$.

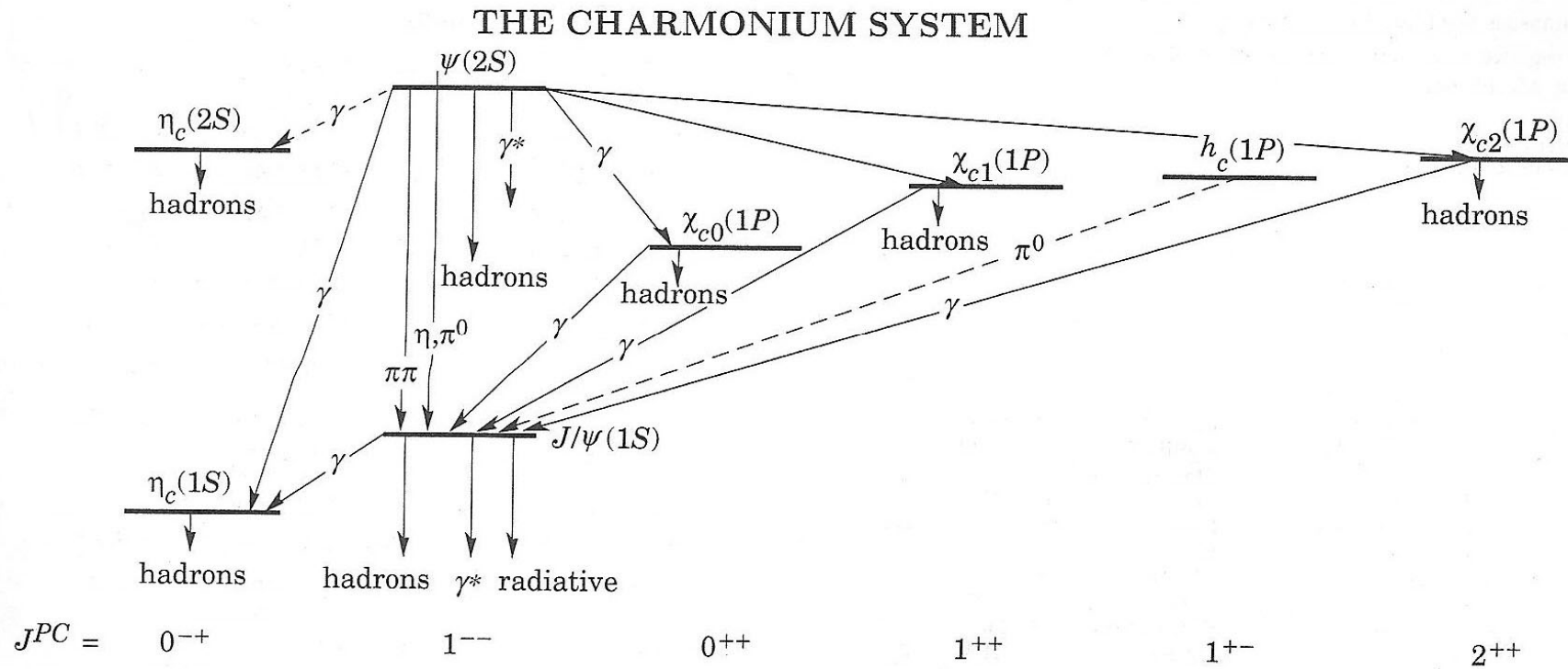


Fig.3. *Top* Mesons of (bb)-structure with radial excitations $n=1$ and $n=1-3$ close to $4m_\pi$ [1,27];
Bottom Mesons of (cc)-structure with radial excitation ($n=1$) close to $4\Delta M_\Delta = 4 \times 147 \text{ MeV} = 588 \text{ MeV}$.

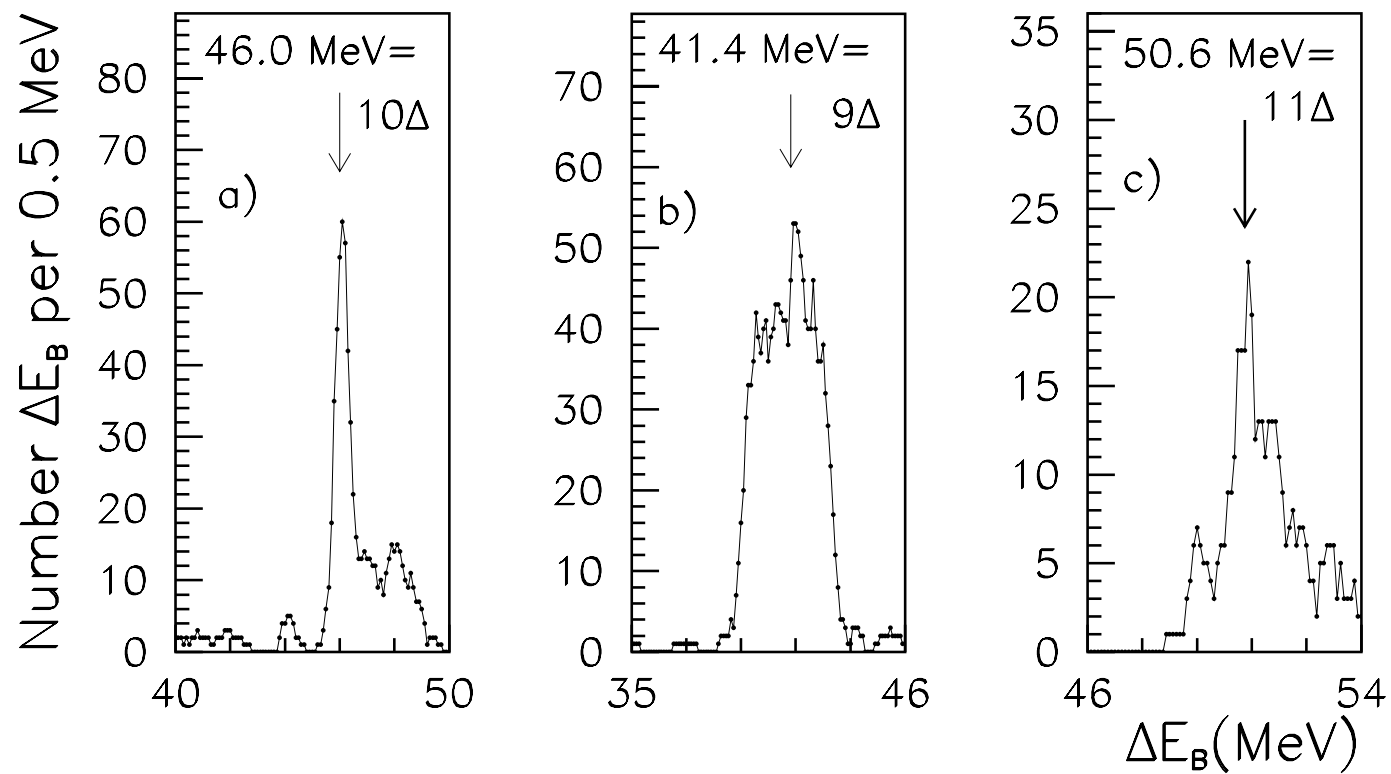


Fig. 4, *Top*: Distribution of ΔE_B in nuclei with $\Delta Z=2$, $\Delta N=4$, $Z=50-58$, $64-82$ and $Z \leq 28$ [26]
Bottom: The same in all even-even and nuclei [26], in even-even nuclei with $Z \leq 58$ [29].

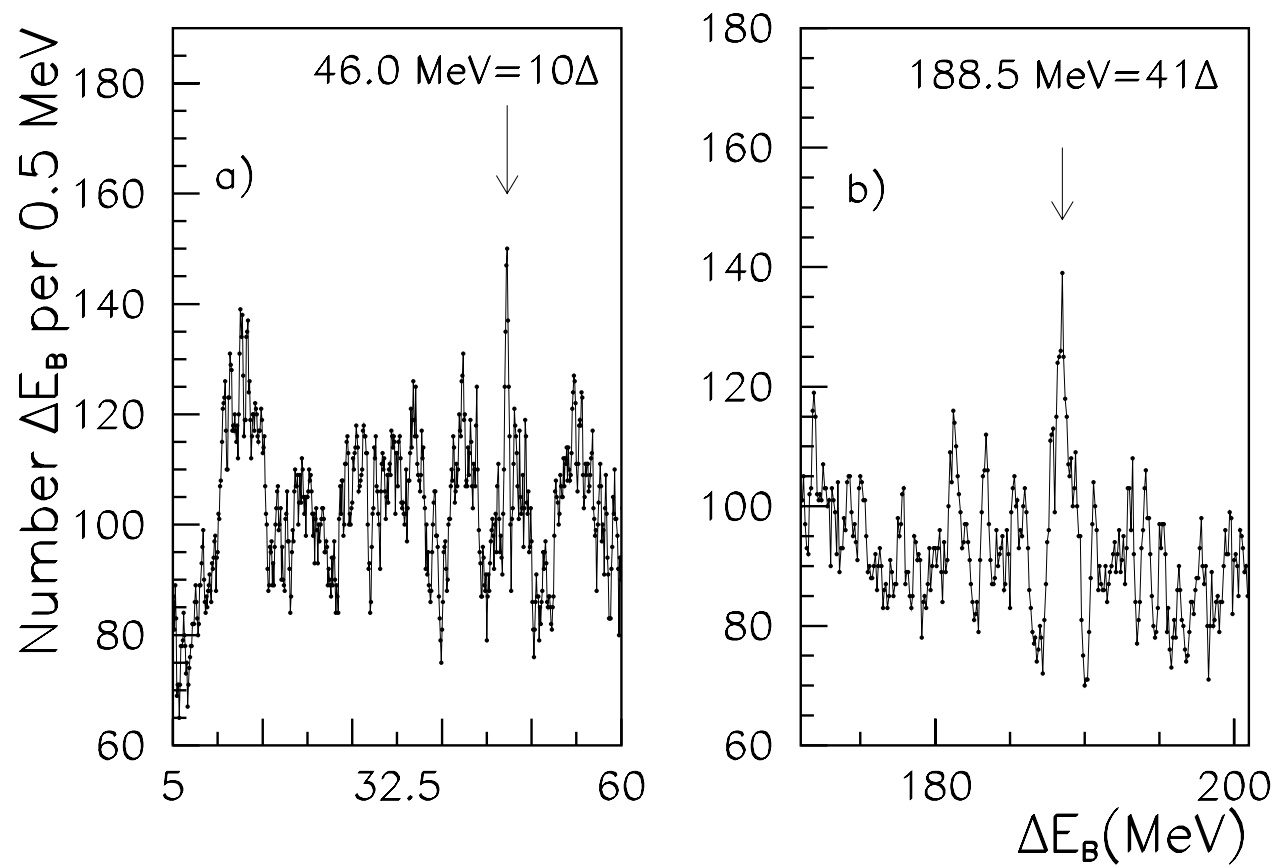


Fig. 4, *Top*: Distribution of ΔE_B in nuclei with $\Delta Z=2$, $\Delta N=4$, $Z=50-58$, $64-82$ and $Z \leq 28$ [26]
Bottom: The same in all even-even and nuclei [26], in even-even nuclei with $Z \leq 58$ [29].

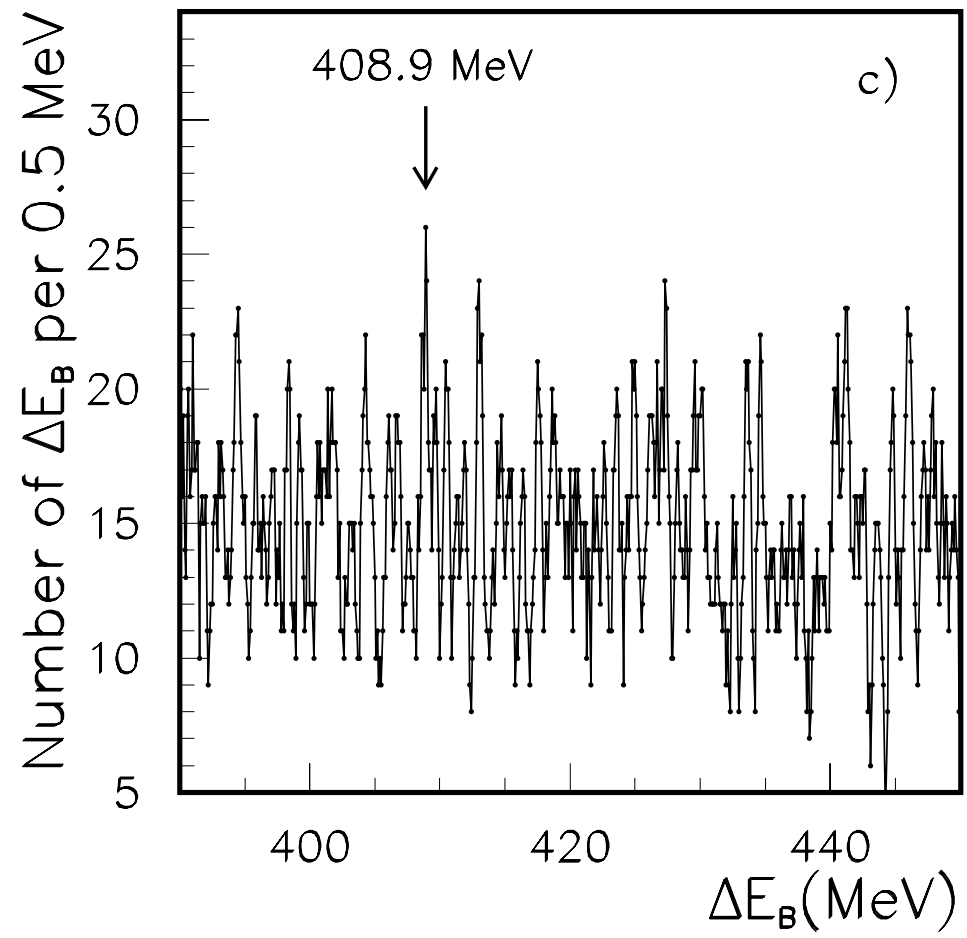
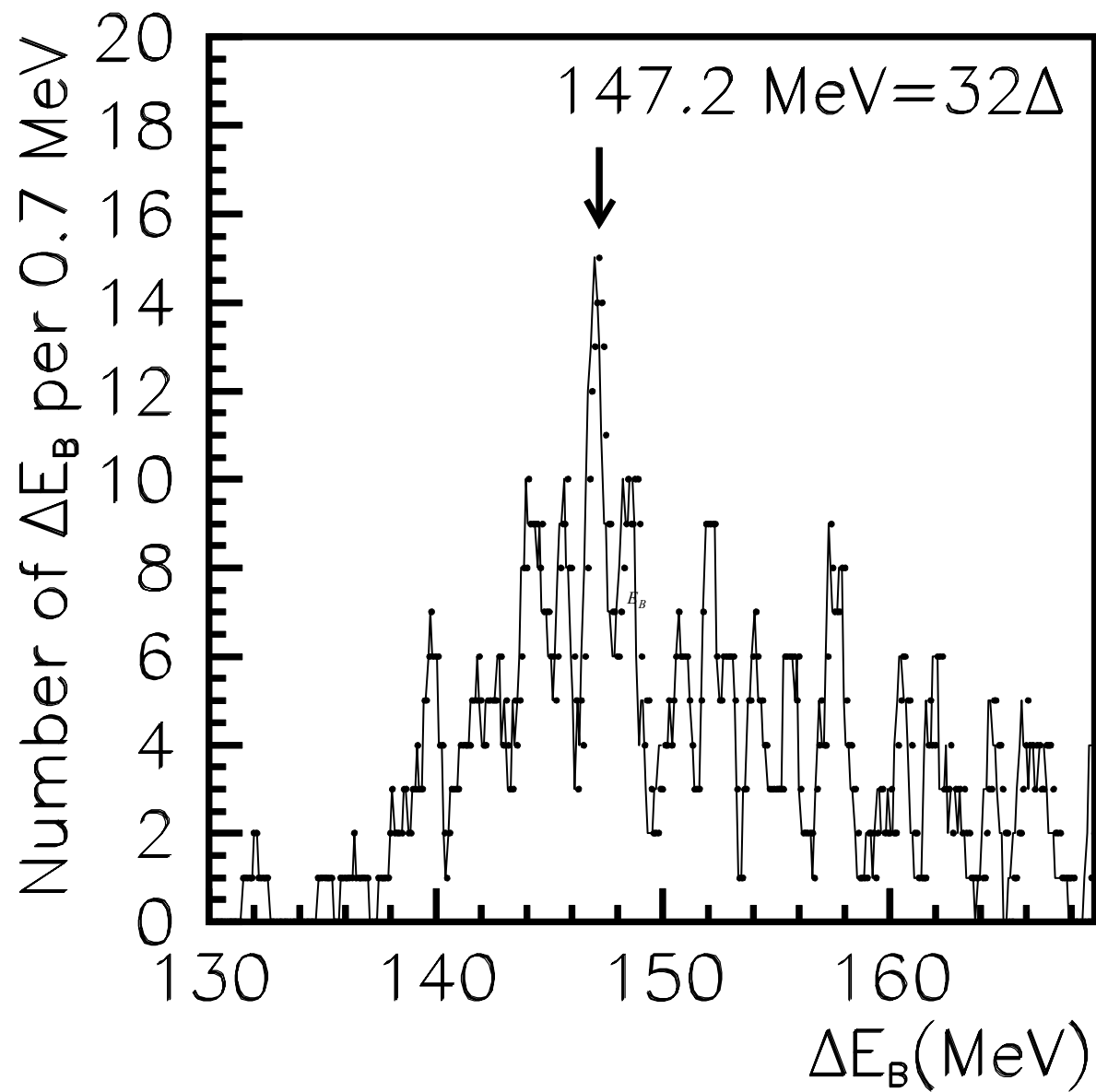
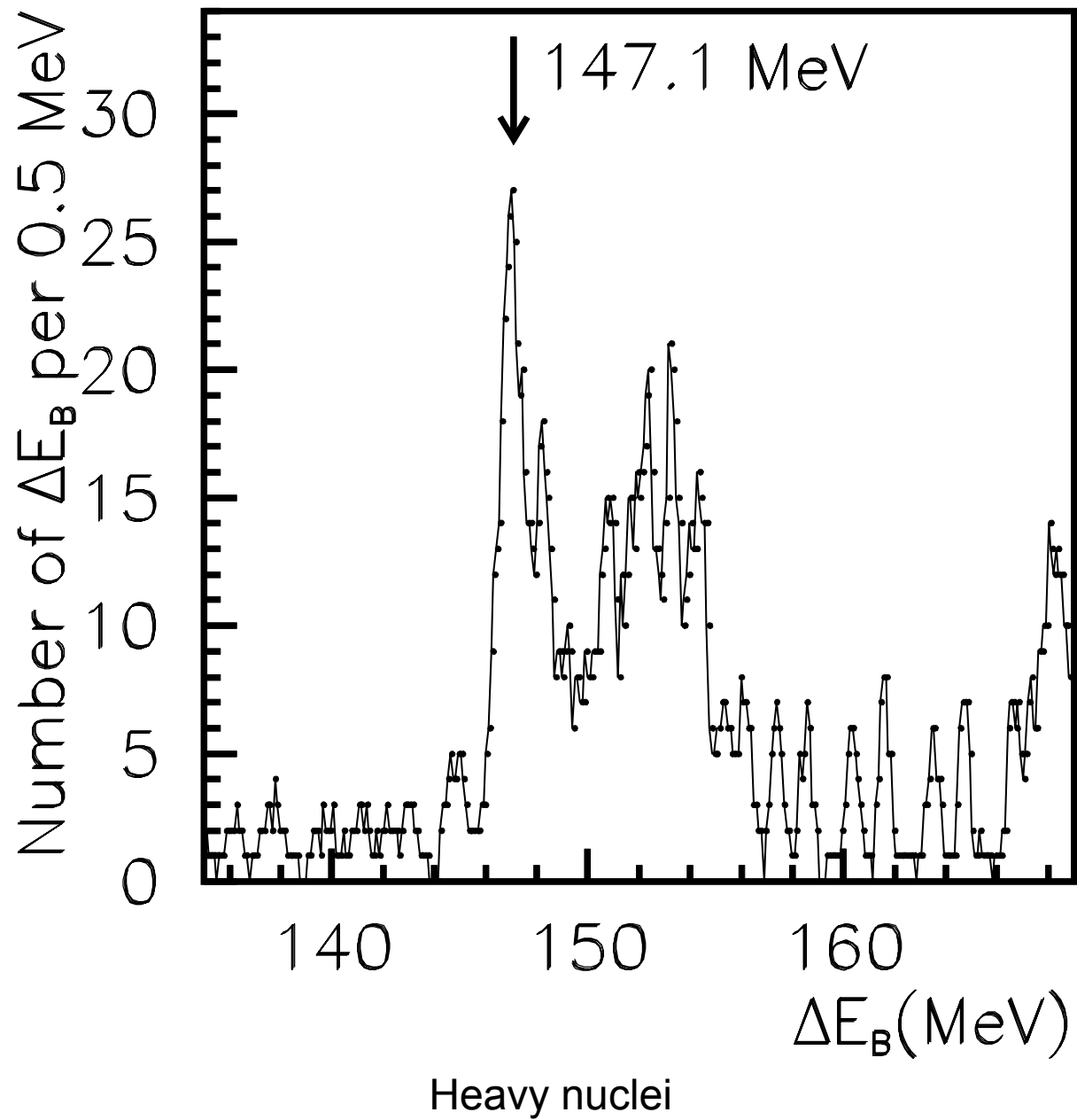


Fig. 4, *Top:* Distribution of ΔE_B in nuclei with $\Delta Z=2$, $\Delta N=4$, $Z=50-58$, $64-82$ and $Z \leq 28$ [26]
Bottom: The same in all even-even and nuclei [26], in even-even nuclei with $Z \leq 58$ [29].



Z less 26

ΔE_B (4 α)



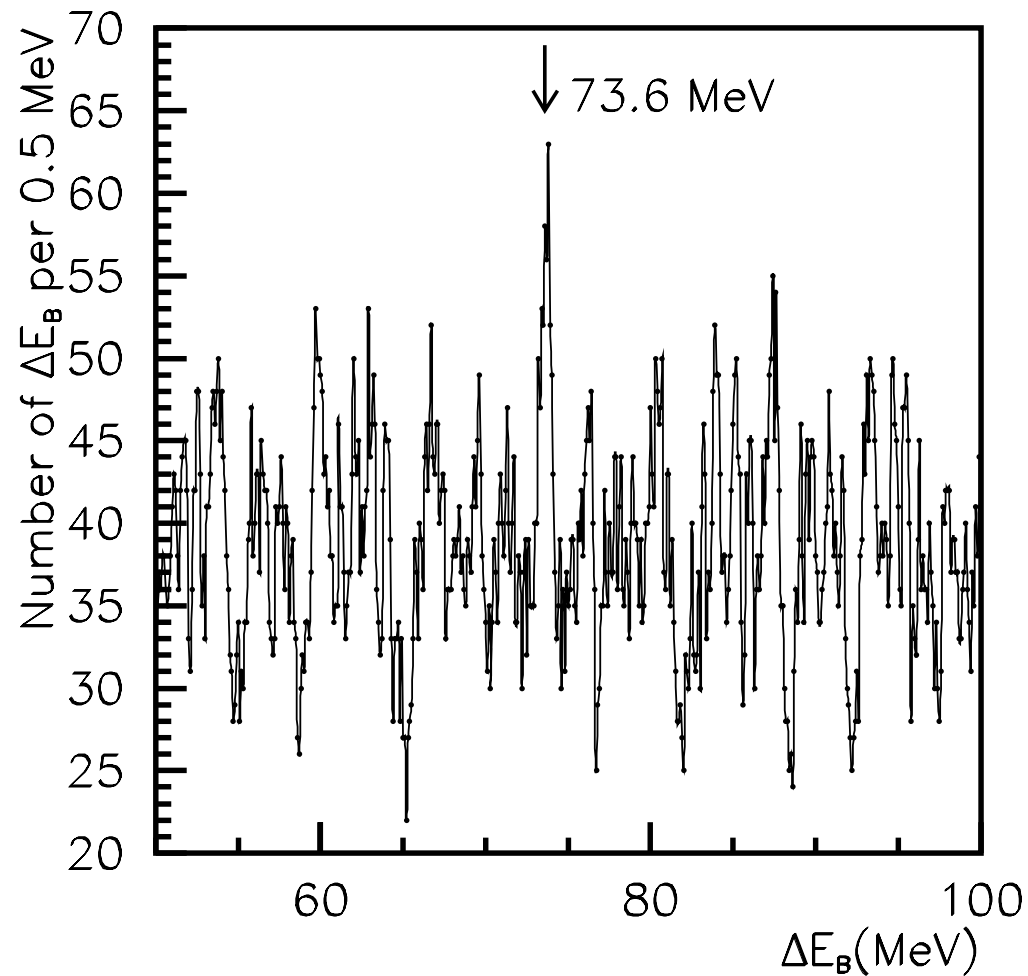


Fig. 5, *top*: Distribution of ΔE_B in nuclei with $\Delta Z \leq 26$; 4α - 2α -config. and all nuclei [6]);
center: Distribution of adjacent intervals ΔE_{B-AIM} in nuclei with $Z \leq 26$ for $x=147.2$ and 73.6 MeV [6]);
bottom: Distribution of ΔE_B in nuclei with $\Delta Z=8$, $\Delta N=14$ ($Z=50-82$); Distribution of ΔE_{B-AIM} in nuclei with $\Delta Z=65-81$ for $x=147.1$ MeV [6]; Distribution of ΔE_B in all odd-odd nuclei [26].

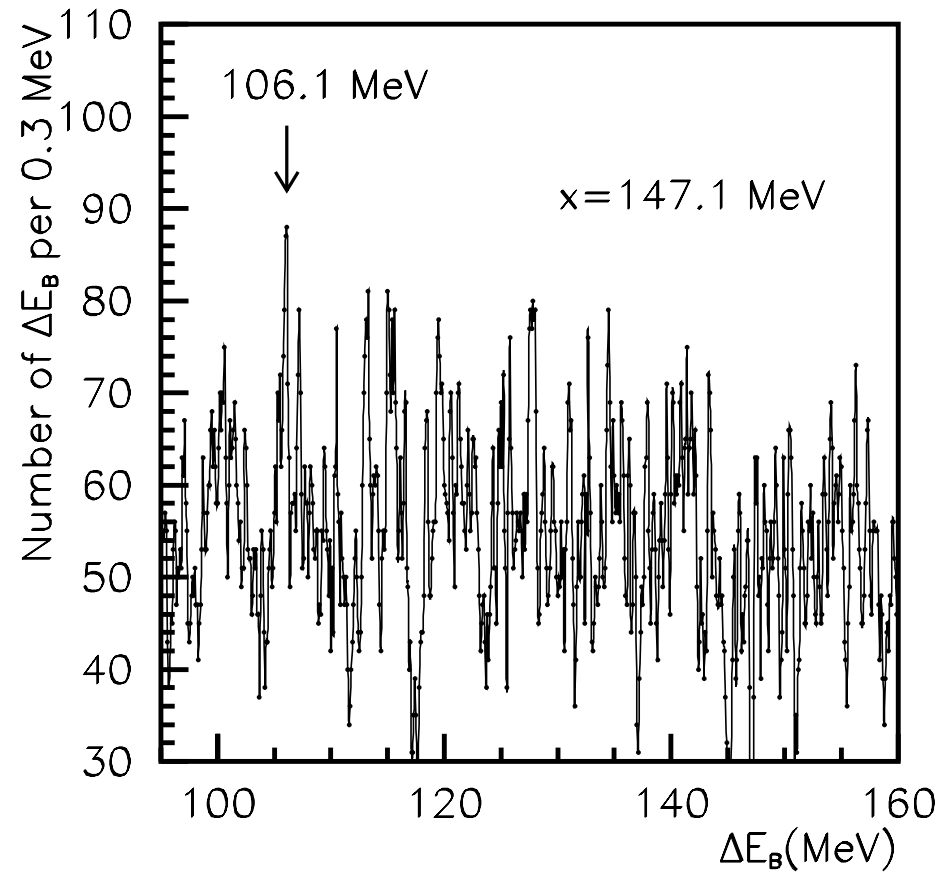


Fig. 5, *top*: Distribution of ΔE_B in nuclei with $\Delta Z \leq 26$; $4\alpha - 2\alpha$ -config. and all nuclei [6]);
center: Distribution of adjacent intervals ΔE_{B-AIM} in nuclei with $Z \leq 26$ for $x=147.2$ and 73.6 MeV [6]);
bottom: Distribution of ΔE_B in nuclei with $\Delta Z=8$, $\Delta N=14$ ($Z=50-82$); Distribution of ΔE_{B-AIM} in nuclei with $\Delta Z=65-81$ for $x=147.1$ MeV [6]; Distribution of ΔE_B in all odd-odd nuclei [26].

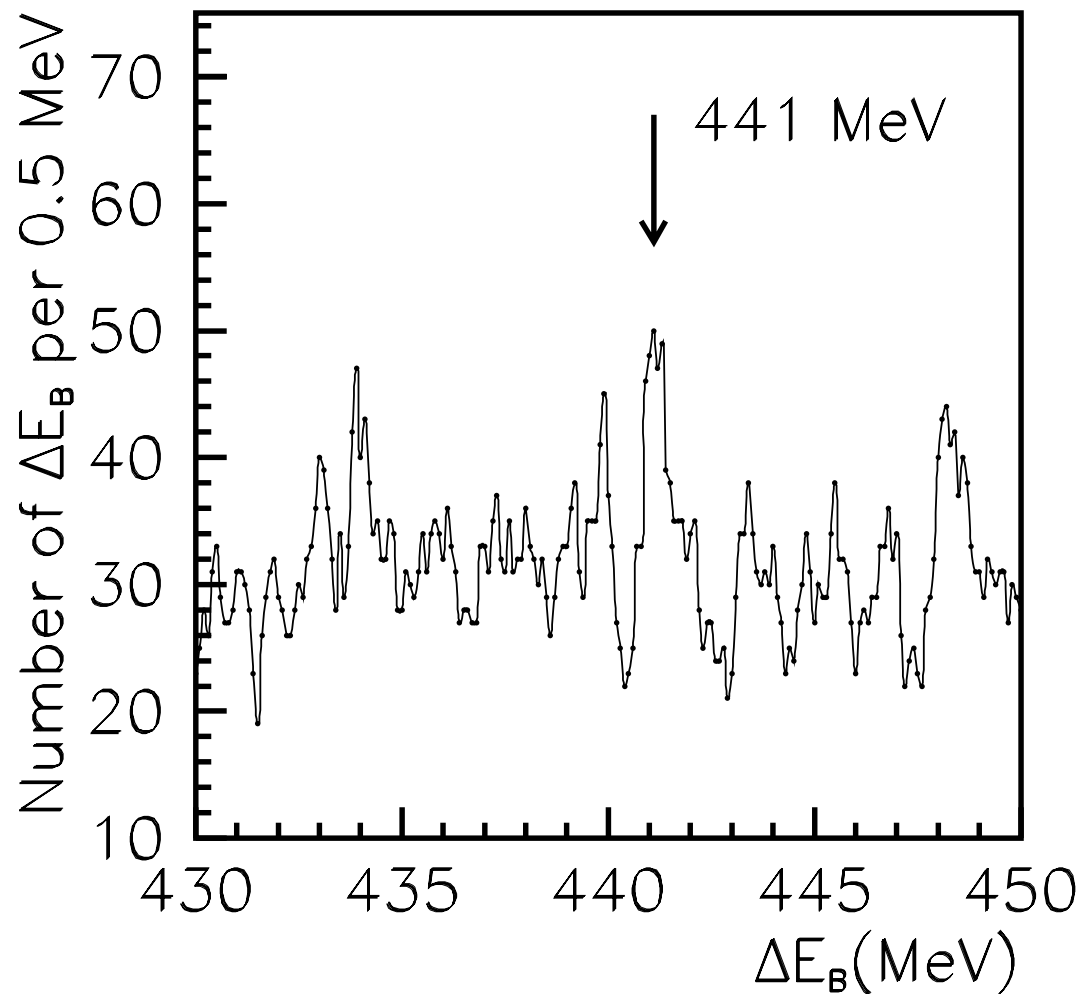


Fig. 5, *top*: Distribution of ΔE_B in nuclei with $\Delta Z \leq 26$; $4\alpha - 2\alpha$ -config. and all nuclei [6]);
center: Distribution of adjacent intervals ΔE_{B-AIM} in nuclei with $Z \leq 26$ for $x=147.2$ and 73.6 MeV [6]);
bottom: Distribution of ΔE_B in nuclei with $\Delta Z=8$, $\Delta N=14$ ($Z=50-82$); Distribution of ΔE_{B-AIM} in nuclei with $\Delta Z=65-81$ for $x=147.1$ MeV [6]; Distribution of ΔE_B in all odd-odd nuclei [26].

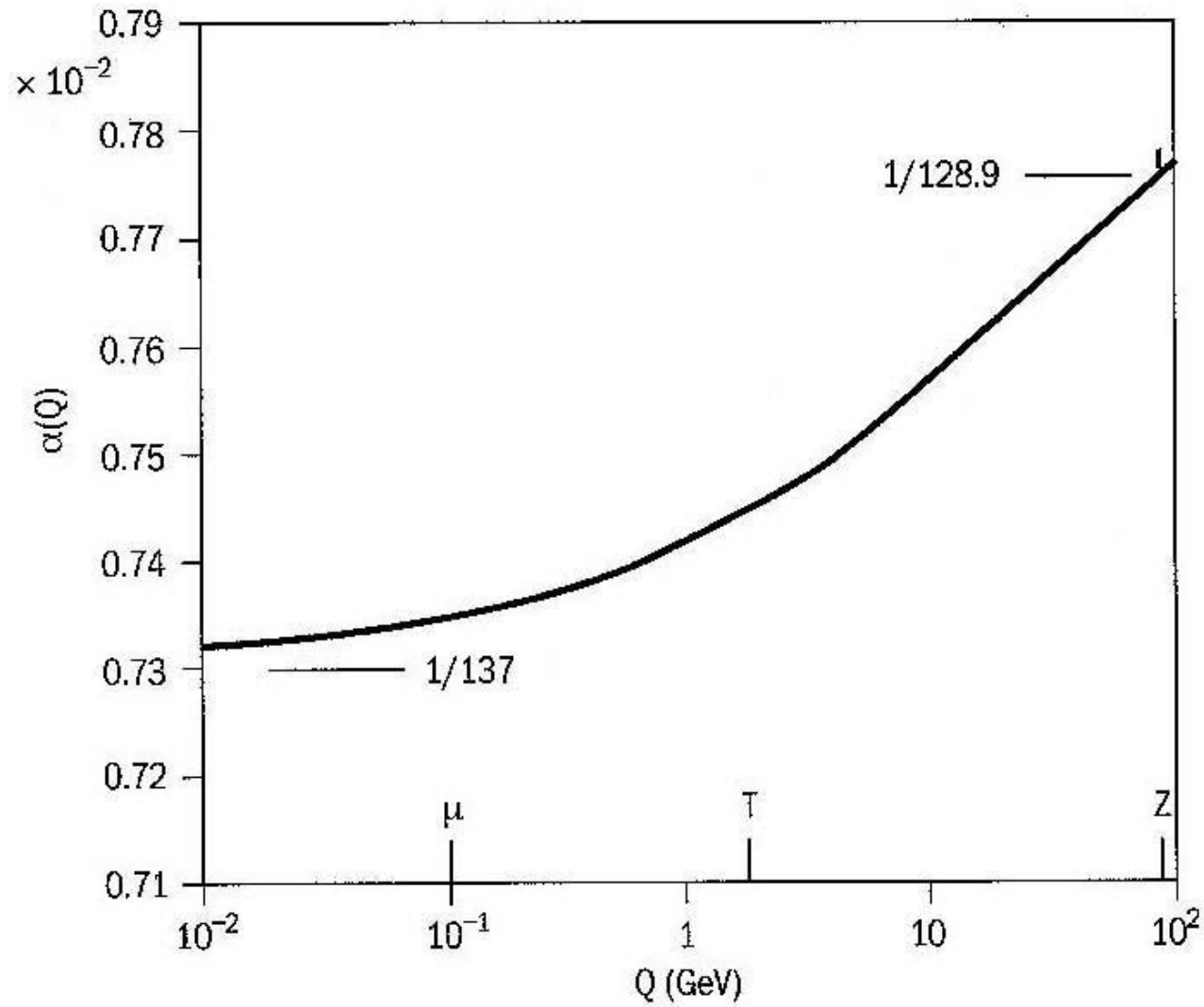


Fig.6. Momentum transfer evolution of QED effective electron charge squared. The monotonically rising theoretical curve is confronted with precise measurements at the Z mass at CERN LEP collider

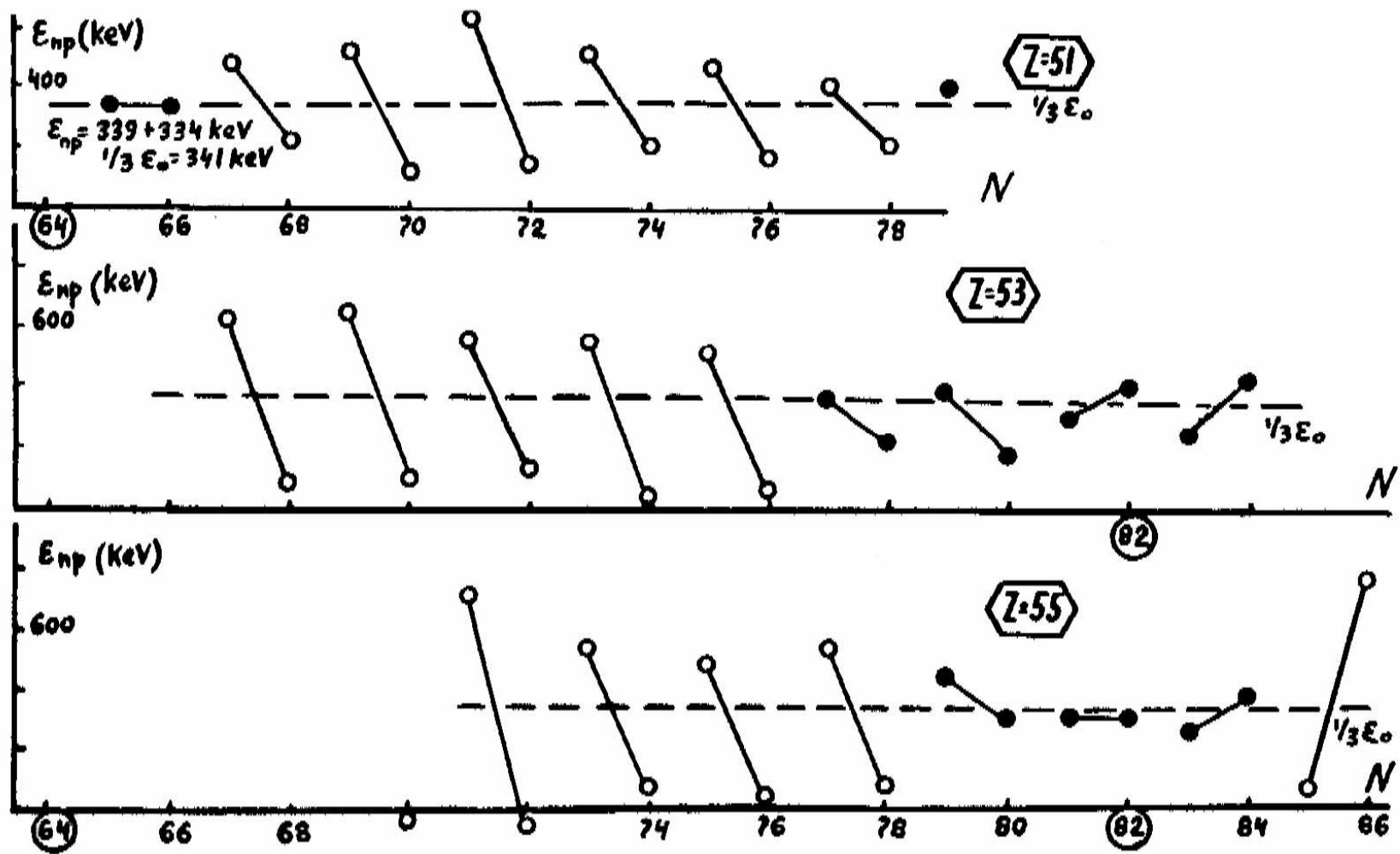
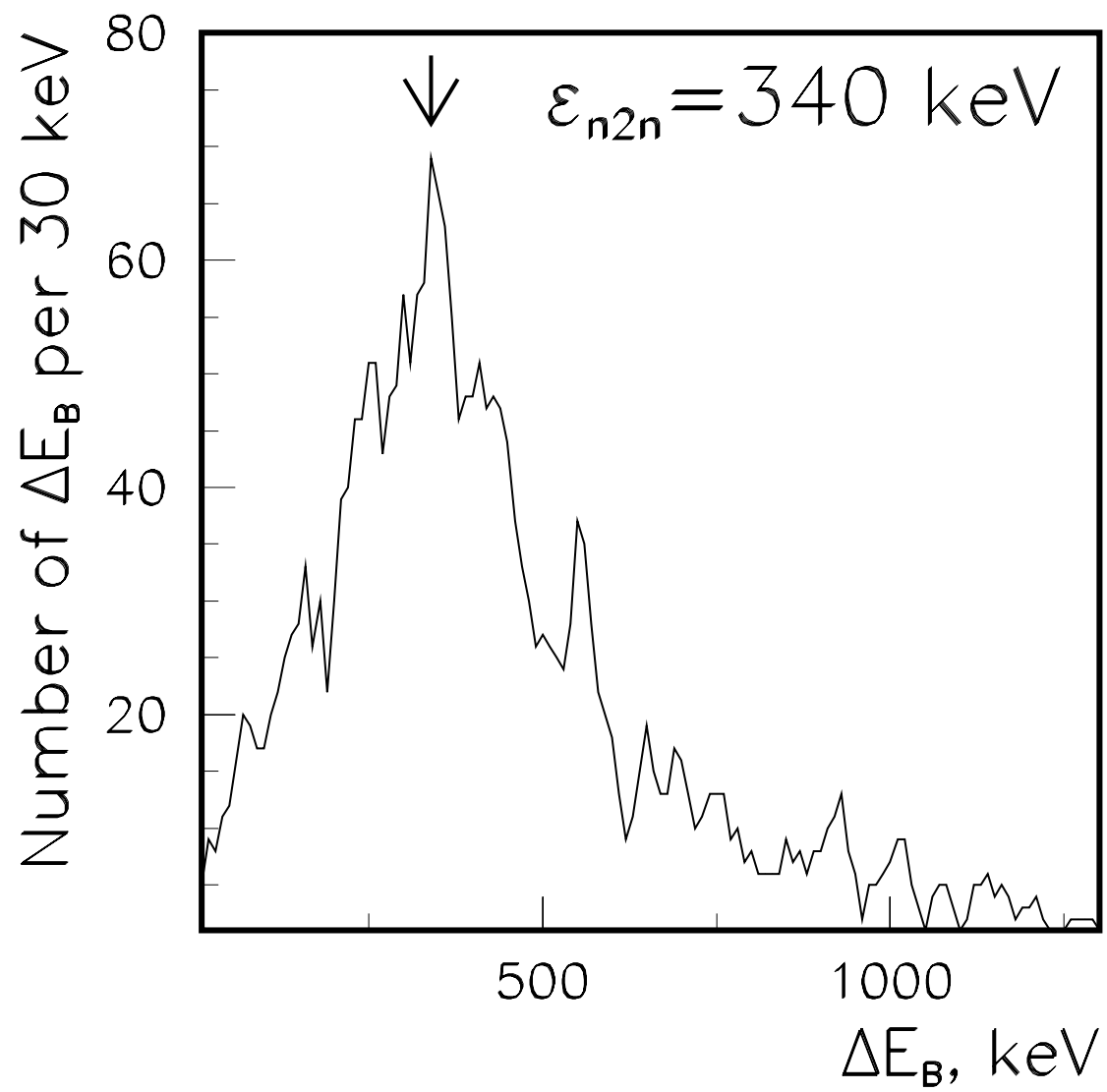
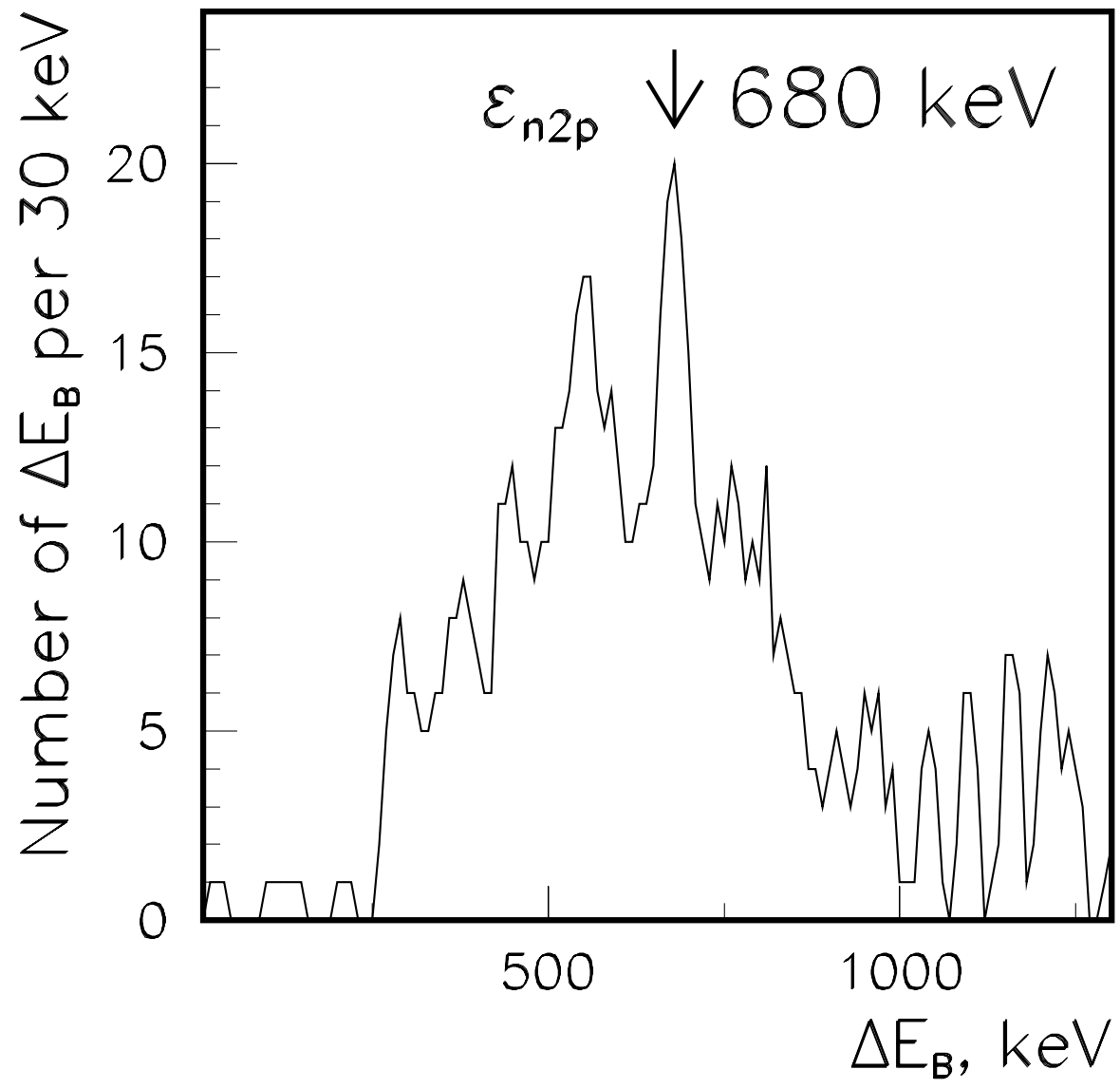
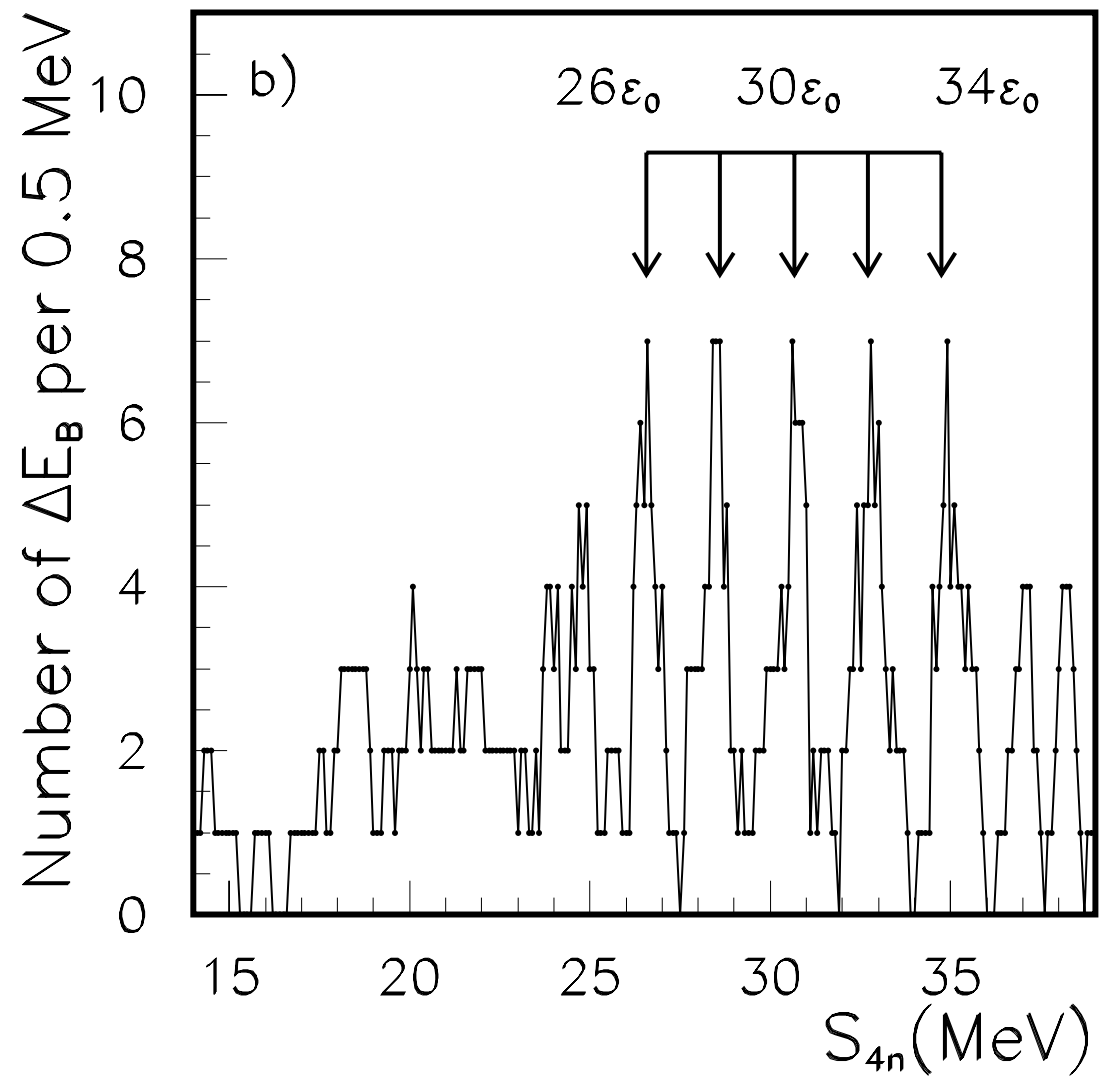
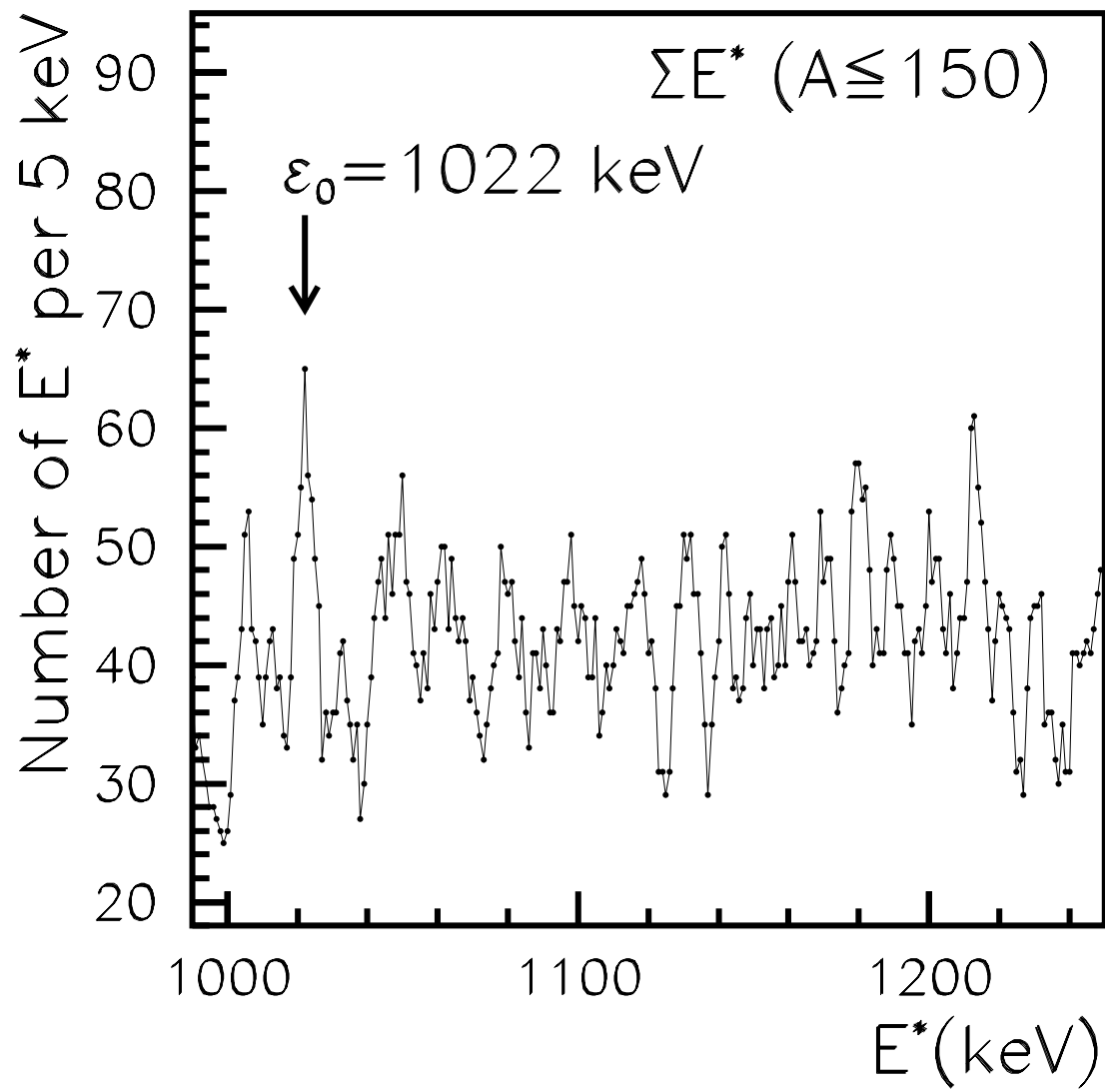


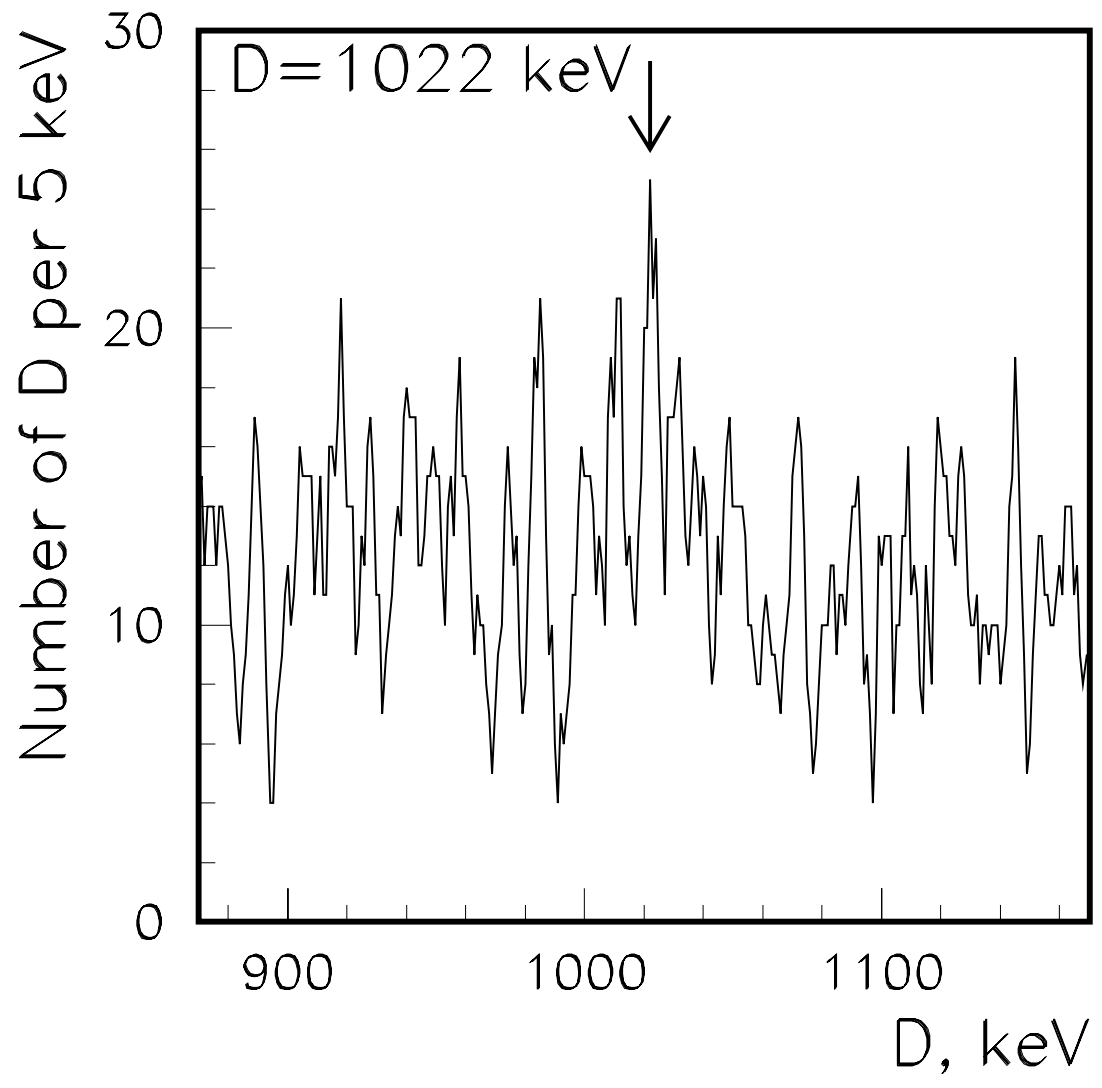
Fig.7. Parameters of the residual interaction ϵ_{np} from differences of S_p in Z -odd nuclei ($\Delta N = 1$). The value $\epsilon_0/3=341$ keV is given by horizontal line

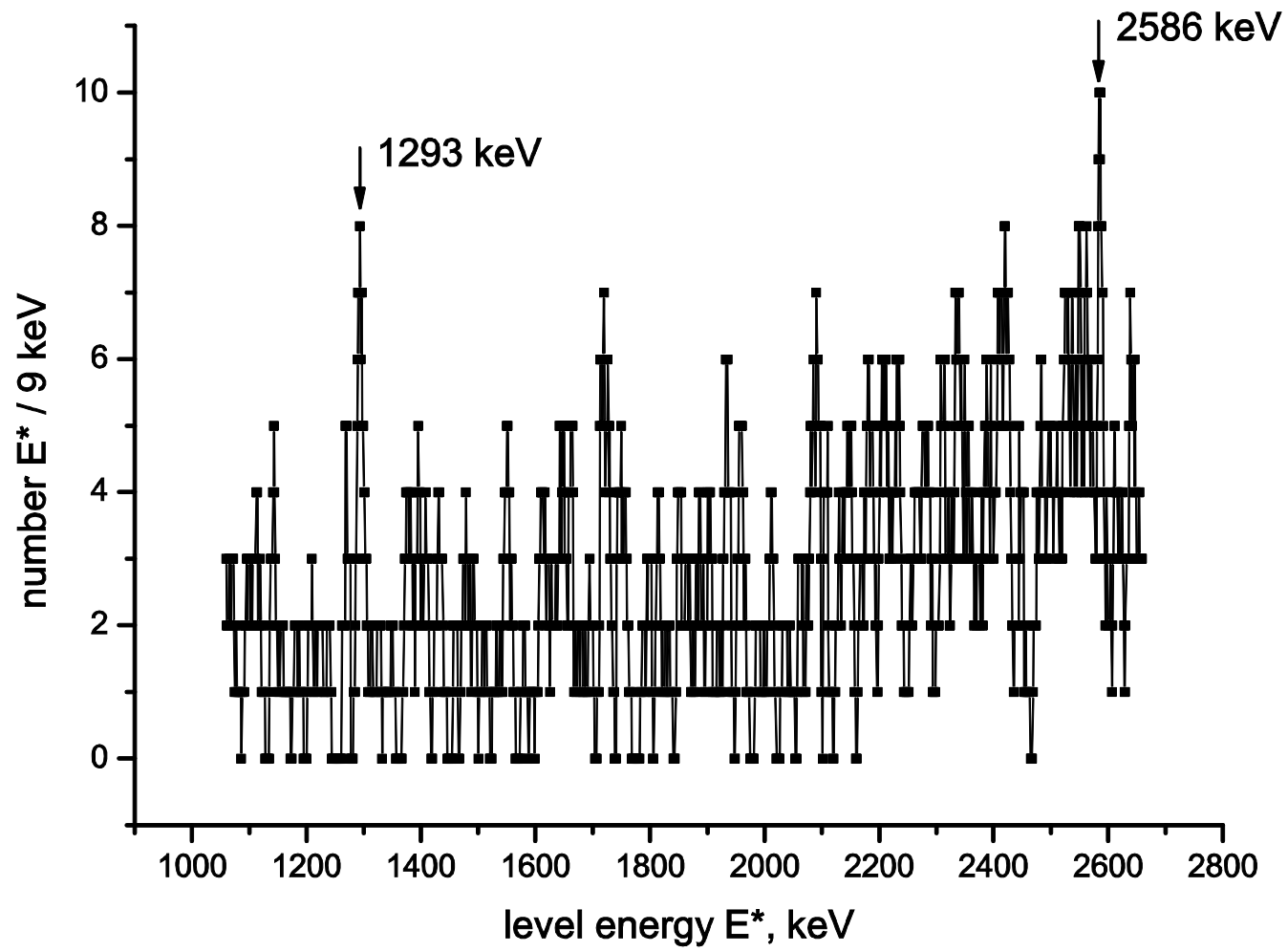


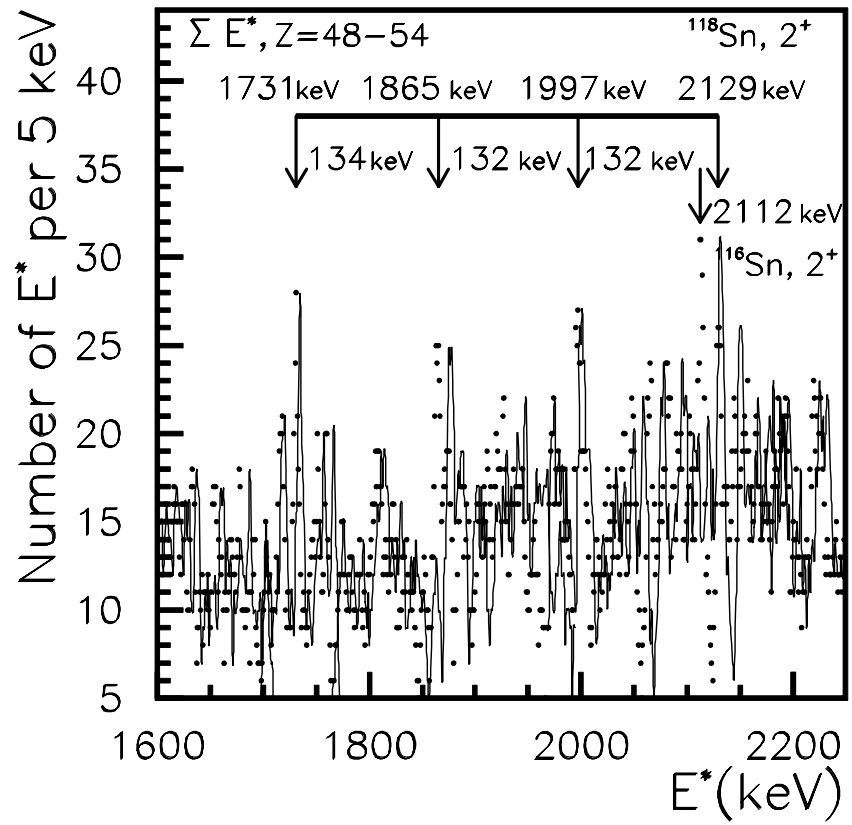
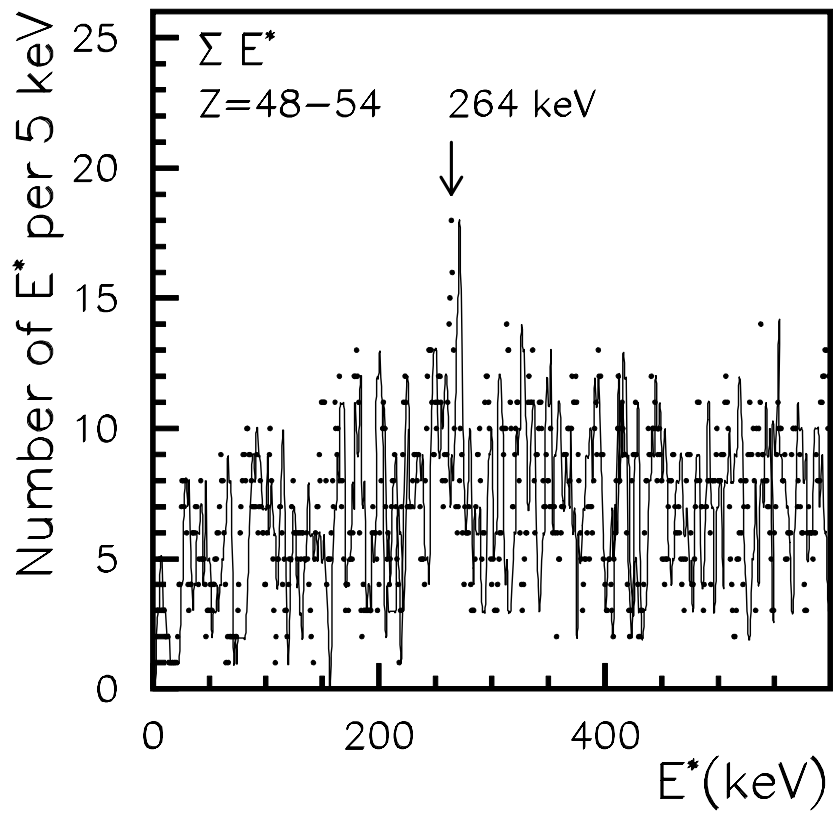


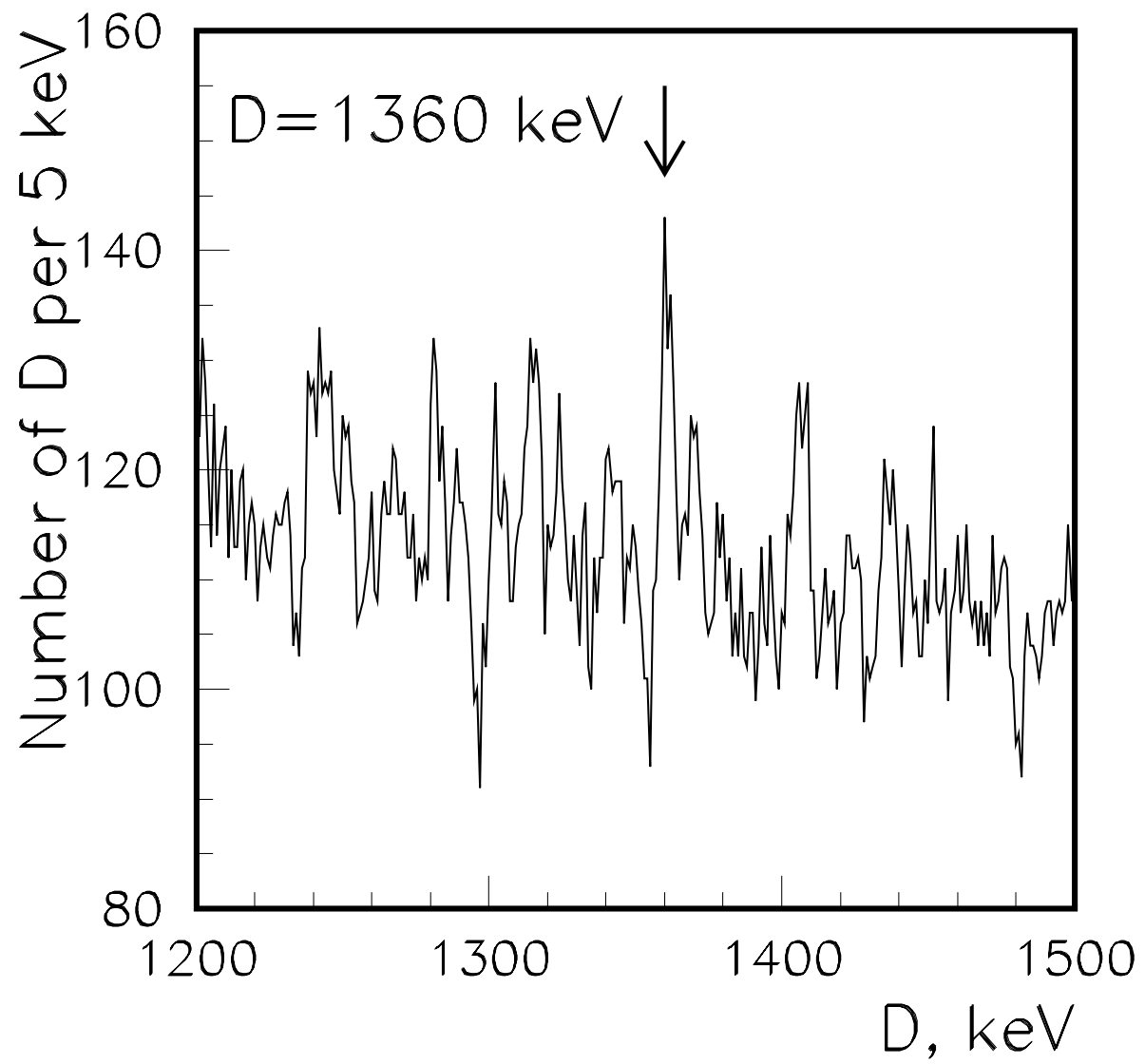


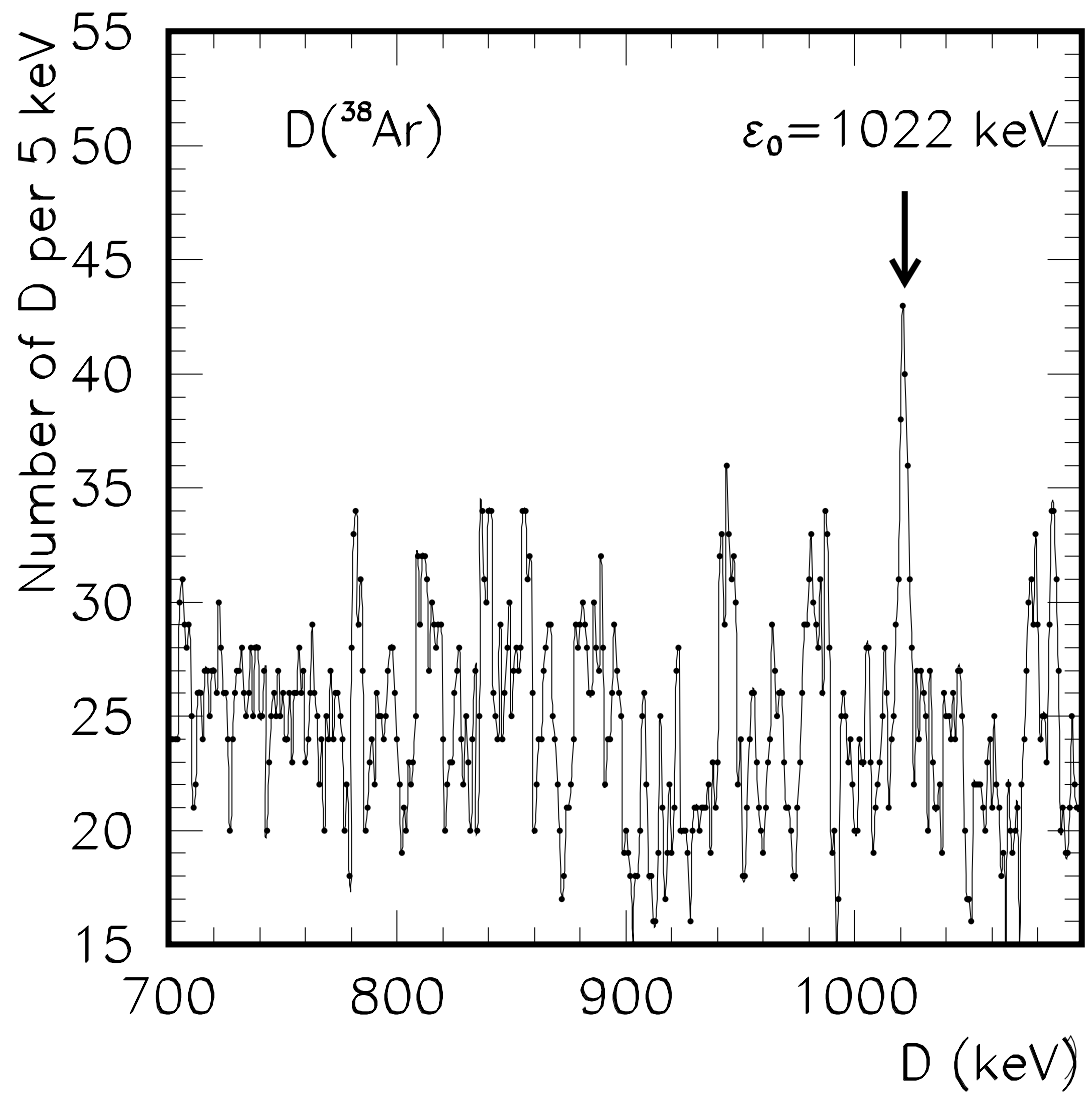


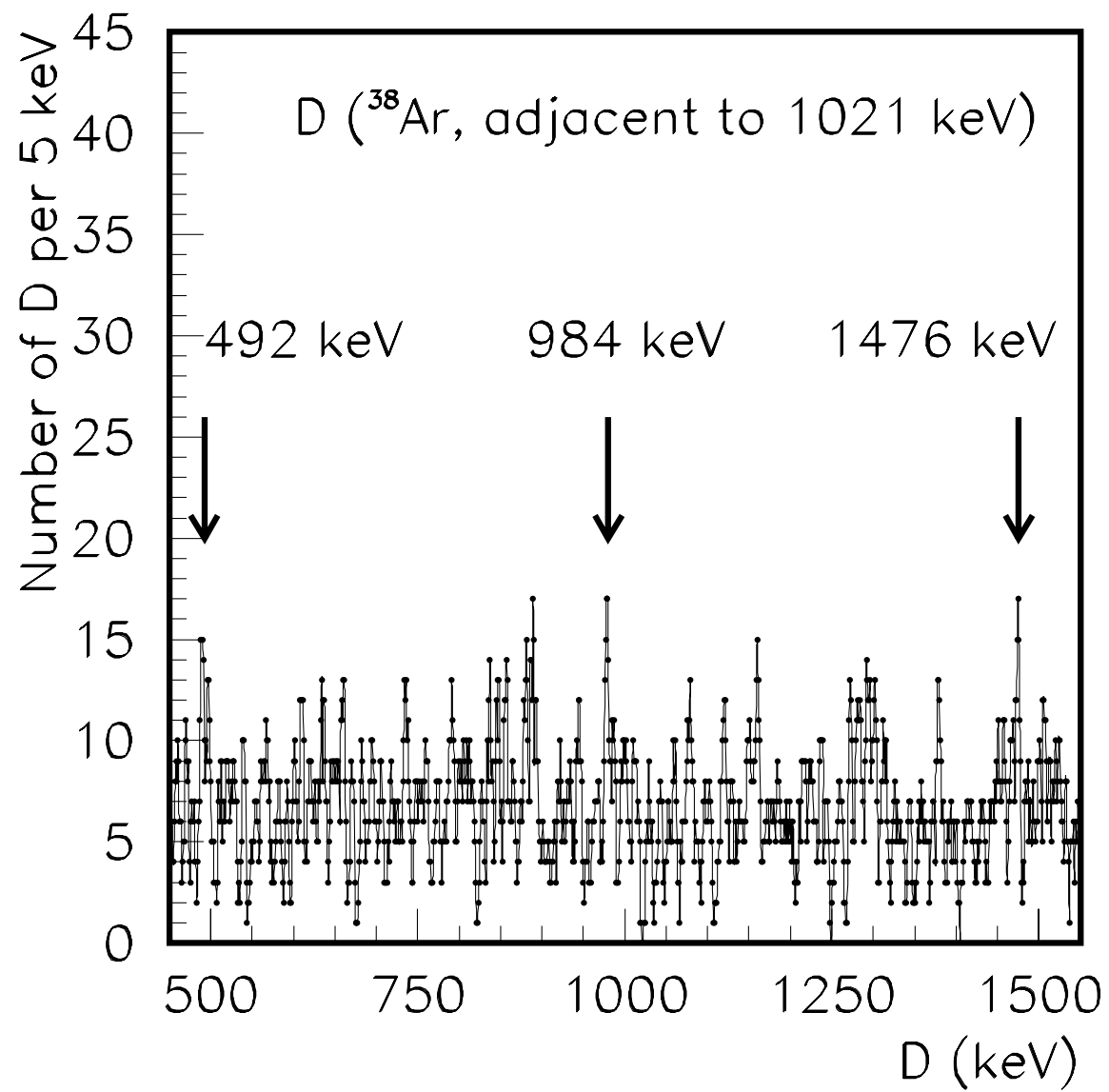


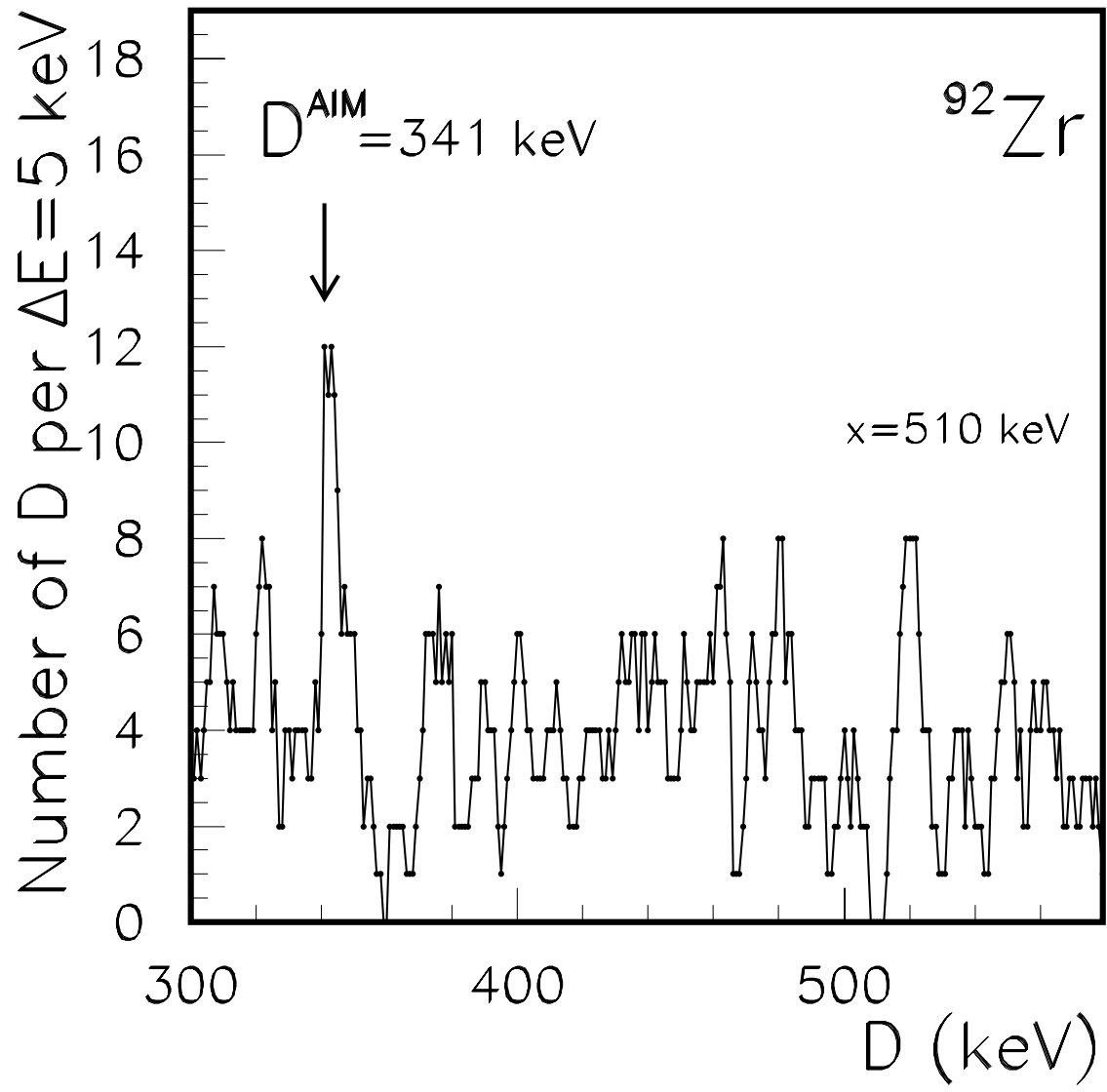












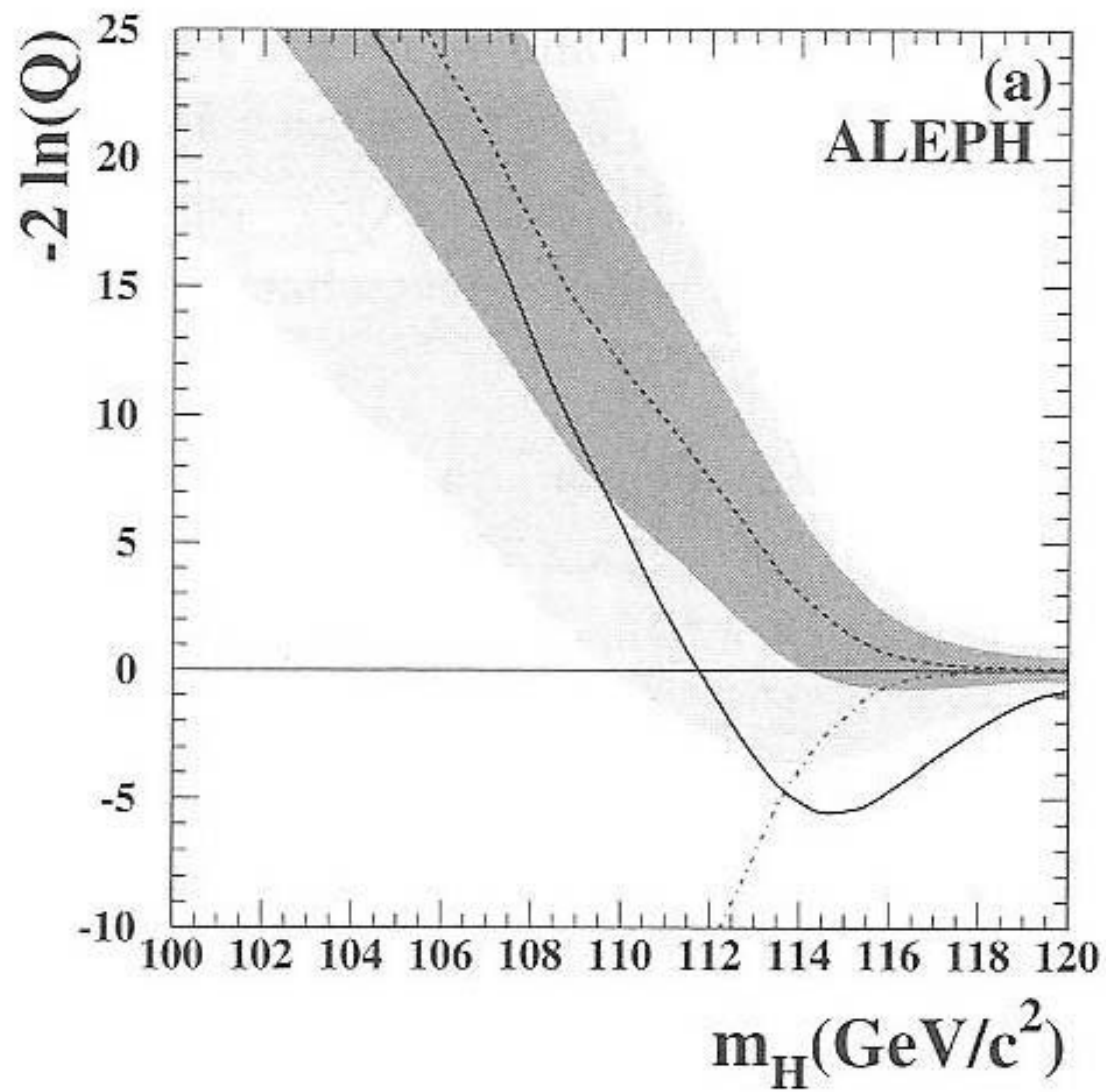


Fig.8. ALEPH results with about 3 standard deviation at mass 115 GeV; observed (solid line) and the expected behaviors of the test statistic (dark region) are presented and discussed in [1].

Table 3. Representation of parameters of tuning effects in particle masses (upper part) and in nuclear data by the expression $(n \times m_e (\alpha/2\pi)^x) \times m$ with $\alpha=137^{-1}$ [5]. Asterisk marks stable intervals observed in low-energy excitations and neutron resonances; $\varepsilon_{np}=340$ keV is discussed in the text, Fig.7

x	m	n=1/8	n=1	n=13	n=16	n=17	n=18
-1	1			$M_Z=91.188$	$M_H=115$		
GeV	3				$2m_t=348$		
0	1	$2m_e$	$16m_e$	$m_\mu=105.658$		$m_\pi-m_e$	$147=\Delta M_\Delta$
MeV	1	ε_o	δ	$106.4=\Delta E_B$	$130=\Delta E_B$	$140=\Delta E_B$	$147=\Delta E_B$
	3				$M''_q=m_\rho/2 \approx m_\omega/2$	$M'_q=420$	$M_q=441=\Delta E_B$
1	1	1.2^*	$9.48=\delta'^*$	123^*	152^*	161^*	170^*
keV	2			246^*	303^*	321^*	$\varepsilon_{np}=340=\varepsilon_o/3$
	3			368^*	455^*	481^*	$511=\varepsilon_o/2$
	8	9.5^*	76^*	$984, \text{Fig.8}$	1212^*	$1293=D_o$	$1360, \text{Fig.8}$
2	1		11^*	143^*	176^*	187^*	D in neutron
eV	4	5.5^*	44^*	572^*		$750 - 1500^*$	resonances

Lepton ratio as the distinguished parameter

Earlier, as a realization of Nambu's suggestion to search for empirical mass relations needed for SM-development, it was noticed in [5,6] that

- 1) the well-known lepton ratio $L=m_\mu/m_e=206.77$ becomes the integer $207=9*23=13*16-1$ after a small QED radiative correction applied to m_e (it becomes $m_\mu/m_e(1-\alpha/2\pi)=207.01$)
 - 2) the same ratio $L=207$ exists between masses of vector bosons $M_Z=91.188(2)$ GeV and $M_W=80.40(3)$ GeV and two above discussed estimates of baryon/meson constituent quark masses $M_q=441$ MeV= $m_\Xi/3=(3/2)(m_\Delta-m_N)$ and $M''_q=m_\rho/2=775.5(4)$ MeV/ $2=387.8(2)$ MeV
- [1] ($M_Z/441$ MeV=206.8; $M_W/(m_\rho/2)=207.3$ [5,6]). The origin of these effects should be considered in the complex analysis of tuning effects in particle masses and in nuclear data [5,6].

Conclusions

The QCD-based estimates of the constituent quark masses ($M_0 q=420$ MeV, $M_q=441$ MeV, M''_q) could play important role in the description of Standard Model dynamics if the observed now empirical relations in particle masses (and value M_H) would be confirmed in the experiment.

Nuclear data can provide some important additional information on fundamental properties of strong nucleon interactions and nuclear matter as well as general properties of fermion systems.